Journal of Power Sources 225 (2013) 323–329

Contents lists available at SciVerse ScienceDirect

Journal of Power Sources

journal homepage: www.elsevier.com/locate/jpowsour

Electrodeposited platinum thin films with preferential (100) orientation: Characterization and electrocatalytic properties for ammonia and formic acid oxidation

Erwan Bertin [a], Sébastien Garbarino [a], Daniel Guay [a,*], José Solla-Gullón [b], Francisco J. Vidal-Iglesias [b], Juan M. Feliu [b]

[a] INRS-Énergie, Matériaux Télécommunications, 1650 Blvd. Lionel-Boulet, C.P. 1020, Varennes, QC, Canada J3X 1S2
[b] Institute of Electrochemistry, University of Alicante, E-03080 Alicante, Spain

HIGHLIGHTS

- Porous and preferentially oriented {100} Pt thin films are prepared.
- The surface of these electrodes is composed of up to 47% of (100) Pt sites.
- The current for the electro-oxidation of ammonia is 4.8 times higher than on polycrystalline Pt.
- The current for the electro-oxidation of formic acid is 2.6 times higher than on polycrystalline Pt.

GRAPHICAL ABSTRACT

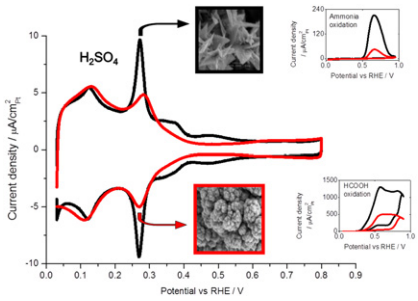

ARTICLE INFO

Article history:
Received 16 July 2012
Accepted 26 September 2012
Available online 27 October 2012

Keywords:
Electrodeposition
(100) surfaces
Bismuth adsorption
Ammonia oxidation
Formic acid oxidation

ABSTRACT

The electrocatalytic activity of preferentially oriented {100} Pt electrodes for the electro-oxidation of ammonia (0.2 M NaOH + 0.1 M NH_3) and formic acid (0.5 M HCOOH + 0.5 M H_2SO_4) was assessed. They were prepared without using any surfactant through potentiostatic deposition (E_d = −0.10 V *vs* RHE, [HCl] = 10 mM and [$Na_2PtCl_6 \cdot 6H_2O$] = 0.5 mM) and by varying the deposition charge. For comparison, polycrystalline Pt thin films were prepared using the same solution but with E_d = +0.10 V *vs* RHE. Quantification of the fraction of (111) and (100) sites was performed by bismuth irreversible adsorption and deconvolution of the hydrogen region, respectively. Samples with as much as 47% of (100) surface sites were obtained. The preferential orientation was further confirmed by CO stripping voltammetry that exhibits similar characteristic features, as well as a similar potential of zero total charge than those expected for a preferential (100) surface. As compared to polycrystalline Pt, the occurrence of Pt (100) surface sites leads to an electrocatalytic activity enhancement by a factor of 4.8 and 2.6 (expressed as μA cm^{-2}_{Pt}) for the oxidation of ammonia and formic acid, respectively.

1. Introduction

Platinum is one of the most studied elements in electrocatalysis and was investigated for several reactions including the electro-oxidation of hydrazine [1], ammonia [2], formic acid [3] and a variety of alcohols [4]. In the last decades, improvements of the activity and the poisoning resistance of platinum-based catalysts have been obtained by increasing the electrochemically active surface area (EASA) and by mixing platinum with various elements to form alloys and core/shell nanostructures [5,6]. Optimization of the EASA was achieved by preparing 0D (nanoparticles) and 1D nanostructures (nanowires and nanotubes), both approaches resulting in an enhancement of the surface to mass ratio [7–13], while improvement

* Corresponding author. Tel.: +1 450 929 8141; fax: +1 450 929 8102.
E-mail address: guay@emt.inrs.ca (D. Guay).

0378-7753/$ – see front matter © 2012 Elsevier B.V. All rights reserved.
http://dx.doi.org/10.1016/j.jpowsour.2012.09.090

of both the activity [14,15] and the resistance to poisoning [16] could be reached by preparing platinum alloys and core–shell structures. Also, these later approaches allow a reduction of the platinum content [17,18] and therefore a reduction of the cost of materials.

More recently, a new approach has started to emerge to improve the performances of a catalyst that consists in the preparation of electrodes with a specific surface crystallographic structure [19]. The impetus to follow that approach comes from several studies on single crystals that have shown that several electrochemical reactions of interest are structure-sensitive. For example, in alkaline medium, the electro-oxidation of ammonia on Pt occurs almost exclusively on surface sites with (100) symmetry [3,20,21]. Likewise, in acidic medium, platinum (100) single crystals have the highest intrinsic activity for formic acid oxidation, even though their resistance to poisoning is lower than onto (111) surfaces [4]. Therefore, careful tuning of the crystallographic surface orientation of an electrode can lead to drastic improvements in the activity, selectivity and stability of the catalyst.

In the early 1970s, experiments made by Arvia's group described an electrochemical method to modify bulk polycrystalline platinum to obtain surfaces with preferential orientation via the use of repetitive potential sweeps at high frequency under carefully-selected potential perturbation conditions [22–24]. However, because of the low roughness factor, even if the electrocatalytic activity, expressed in terms of current per Pt surface atom, was high, the resulting activity, expressed in current per geometric surface area, was low [22]. More recently, platinum nanoparticles with a preferential orientation were successfully prepared, exhibiting both a specific surface structure and a high EASA [25]. This was achieved using a capping agent, sodium polyacrylate, and hydrogen gas as a reducing agent. High resolution transmission electron microscopy confirmed that cubic Pt nanoparticles were obtained with (100) facets [26]. Further confirmation of the specific surface orientation was obtained by other groups as these nanoparticles exhibit characteristic hydrogen adsorption/desorption peaks [27], as well as a second peak during CO stripping experiments [28,29], and clear oxidation response of germanium adsorbed on platinum (100) sites [27]. However, the preparation of these shape-controlled nanoparticles by colloidal methods implies the use of organic ligand stabilizers, which can be challenging to remove without altering the surface orientation of the particles. In contrast, it was shown that electrodeposition can allow the preparation of platinum surfaces with a preferential (100) orientation without the use of surfactants, assuming that the deposition parameters have been carefully set [30,31]. This method, as the colloidal methods, allows the preparation of electrodes with a specific crystallographic surface structure and a high electrochemically active surface area, both in the form of thin films or nanowires, using a template-assisted deposition method in that later case [31].

In the present study, highly {100} oriented Pt thin films were prepared by electrodeposition. The deposition charges used in the preparation of the films were varied. The occurrence of (100) surface sites was assessed through a semi-quantitative analysis of cyclic voltammetric and CO stripping curves. The fraction of (100) and (111) surface sites was quantitatively assessed by deconvolution of the hydrogen desorption region and an analysis of the bismuth redox peaks, respectively. The results will then be correlated with the electrocatalytic activity of the electrodes for the oxidation of ammonia and formic acid. It will be shown that an increased fraction of (100) surface sites leads to an improvement of the electrode activity for both reactions.

2. Experimental

Platinum thin films were prepared by electrodeposition on titanium substrate (Alfa Aesar, 99%, 0.2 mm) pretreated according to the procedure described elsewhere [32]. The electroplating solution consisted of 10 mM HCl (Fisher Scientific, ACS) and 0.5 mM $Na_2PtCl_6 \cdot 6H_2O$ (Alfa Aesar). All depositions were achieved under potentiostatic conditions using a VMP3 multipotentiostat (BioLogic), with the deposition potential referred to the reversible hydrogen electrode (RHE). After deposition, the samples were rinsed with de-ionized water (Millipore, specific resistivity 18.2 MΩ cm).

Electrochemical characterization was performed in a standard two-compartment cell using the RHE as reference electrode and a platinum wire as a counter electrode. A Luggin capillary was used to minimize the iR drop. Prior to the measurements, all glassware and cells were cleaned by first immersion in potassium permanganate solution overnight, and then rinsed with water and a solution of hydrogen peroxide in sulfuric acid. Finally, the glassware and the cells were thoroughly rinsed with de-ionized water, boiled for 30 min and rinsed again several times with de-ionized water. All solutions used were de-aerated using argon (N50, Air Liquid).

The electrochemically active surface area (EASA, expressed as cm^2_{Pt}) was determined from integration of the hydrogen desorption region (after subtraction of the double layer contribution) measured in 0.5 M H_2SO_4 Fisher Scientific, Trace Metals Grade, considering that the charge associated with one monolayer of hydrogen adsorbed on platinum is 230 μC cm^{-2}_{Pt} [33].

Bismuth irreversible adsorption was performed in a saturated bismuth solution (Bi_2O_3, Sigma Aldrich, 99.999%) in 0.5 M sulfuric acid. After adsorption, Bi was oxidized at the Pt surface by scanning the electrode potential from 0.03 V to 0.75 V at 5 mV s^{-1}. The subsequent deconvolution of the hydrogen desorption region was performed with MagicPlot Student 1.5 using Lorentzian peak profile [27].

Carbon monoxide (N47 Air Liquid) adsorption was performed by bubbling CO gas in the electrolyte whilst the potential of the electrode is held constant at 0.15 V. This was done during 3 min, before the excess of dissolved CO was removed by bubbling Ar in the electrolyte for 30 min. Following that, three successive CO stripping voltammograms were recorded at 5 mV s^{-1} between 0.03 and 0.80 V.

Formic acid (Merck 98–100%, pro analysis) oxidation was done in 0.5 M HCOOH + 0.5 M H_2SO_4. The oxidation of ammonia was performed in 0.05 M $(NH_4)_2SO_4$ (Merck, Pro analysis) + 0.2 M NaOH (Merck, Pro analysis). The ohmic resistance (iR drop) was evaluated from the high frequency (~100 kHz) intercept of the impedance spectrum (Nyquist plot, recorded at 0.56 V, in the double layer region) with the horizontal axis.

3. Results and discussion

3.1. Electrochemical characterization of the deposits

The experimental conditions required to prepare electrodeposited Pt thin films that are both highly porous and with a preferential {100} orientation are now well established [31]. The cyclic voltammogram (CV) in 0.5 M H_2SO_4 of a few typical examples are shown in Fig. 1 for Pt thin films prepared at a deposition potential, $E_d = -0.10$ V and low (0.5 mM) platinum salt concentration but variable deposition charges, Q_d, together with the electrochemical response of a polyoriented Pt thin film prepared at $E_d = +0.10$ V. In the lower potential range, the hydrogen desorption region displays three characteristic peaks (h_1–h_3) located at 0.13, 0.26 and 0.35 V that are associated with (110) sites, (100) steps, and (100) terraces, respectively [31]. A fourth additional peak, h_4, is observed at 0.48 V and is related to sulfate adsorption on wide (111) domains.

A qualitative assessment of preferential orientation in Pt thin films can be reached by looking at the relative intensity of h_1–h_3, and calculating the peak current ratio h_2/h_1. Thus, it was

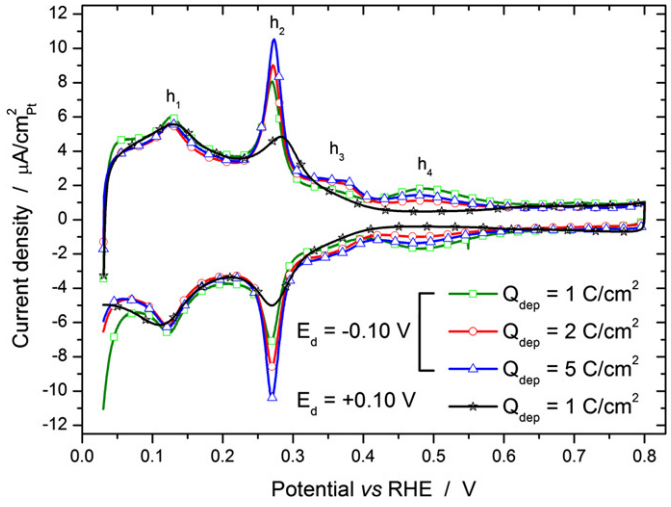

Fig. 1. Cyclic voltammograms recorded at 5 mV s^{-1} in 0.5 M H_2SO_4 of Pt thin films prepared at $E_d = -0.10$ V, using an electrolyte with 10 mM HCl and 0.5 mM $Na_2PtCl_6 \cdot 6H_2O$. The deposition charge is 1, 2 and 5 C cm^{-2} (open squares, open circles and open triangles, respectively). For comparison, the CV of polycrystalline Pt prepared at $E_d = +0.10$ V (stars, the deposition charge is 1 C cm^{-2}) is also shown.

established elsewhere that the ratio h_2/h_1 increases from a value of *ca.* 0.8 for polycrystalline Pt, to more than 2.0 as the relative proportion of (100) step sites increases [31,34]. In some cases, the h_2/h_1 ratio increase is accompanied by a clear contribution at 0.35 V (h_3 attributed to (100) terraces) and a broad peak at 0.48 V (h_4 attributed to wide (111) domains) [35]. In contrast, for polycrystalline Pt, the current peaks h_3 and h_4 are hardly distinguishable [36]. In the present study, a more quantitative approach was used to assess the relative proportion of the various surface crystallographic orientations and how they are influenced by the deposition charge, Q_{dep}. This was achieved by performing a deconvolution of the hydrogen desorption region and from the oxidation of adsorbed Bi according to the procedure developed by Solla-Gullón and co-workers [27].

First, using relation (1), the fraction of (111) terraces, q^t_{111}, was determined from integration of the bismuth oxidation peak at 0.62 V *vs* RHE [37].

$$q_{Bi} = (0.64 \pm 0.02) q^t_{111} \quad (1)$$

The deconvolution of the hydrogen desorption region is slightly more complex and is illustrated in Fig. 2. Details about the procedure, such as the choice of the peak profile and the determination of the peak potentials can be found elsewhere [27]. Briefly, from the CV of the sample recorded at low scan rate in 0.5 M H_2SO_4 (Fig. 2A), the contribution of the double layer is removed. Then, the contribution of the (111) sites (Fig. 2B), estimated from the oxidation of adsorbed Bi atoms and equation (1), is removed using the Pt (554) single crystal surface as a model (Fig. 2C). The deconvolution of the resulting CV (Fig. 2D) is then performed between 0.09 and 0.40 V *vs* RHE using MagicPlot Student 1.5 and Lorentzian peak profile, with 6 different peaks at 0.126, 0.210, 0.257, 0.272, 0.338, and 0.372 V for Pt oriented samples. From studies on single crystals, the contributions at 0.126 and 0.210 V are attributed to low-coordination sites such as kink sites or (110) domains. The anodic contribution at 0.257 V is attributed to (100) step sites on (111) terraces. The peak at 0.272 V is attributed to short (100) terraces, whereas the peaks at 0.338 and 0.372 V are attributed to wide (100) terraces [27]. In the case of polycrystalline Pt, there is no significant amount of (100) terraces, i.e. no contribution at 0.338 and 0.372 V. So, only 5 contributions are considered at 0.126, 0.210, 0.257, 0.272 and 0.290 V, the last peak being associated with the small fraction of (100) terraces present on such Pt thin films. Following the work reported earlier by Feliu and coworkers, the incertitude on the measurement is ±3% [27].

As explained previously, the first step in the determination of (111) surface sites involves the spontaneous adsorption of Bi ions from the electrolyte. The Pt thin films studied in this work have roughness factors, R_f, defined as the ratio between the EASA and the geometric surface area, that can exceed 480. However, for samples with EASA exceeding *ca.* 76 cm^2_{Pt} (corresponding to $R_f = 76$), it was not possible to reach a full coverage of the electrode surface even after fourteen days of immersion in a saturated Bi_2O_3 solution in 0.5 M H_2SO_4. Indeed, for samples with EASA >76 cm^2_{Pt}, the hydrogen desorption region is still discernable after two weeks. As a consequence, a precise determination of the proportion of (111) surface sites could not be reached for Pt samples with an EASA exceeding *ca.* 76 cm^2_{Pt}. This corresponds to Pt deposits ($E_d = -0.10$ V) prepared with a deposition charge of 10 C cm^{-2}. Consequently, this study will focus on Pt surfaces with low R_f values.

The variation of the various crystallographic orientations as a function of Q_{dep} is shown in Fig. 3A. The total fraction of (100) sites (steps and terraces) increases linearly from 27 to 42% as Q_{dep} varies from 0.5 to 4 C cm^{-2}. For $Q_{dep} > 4$ C cm^{-2}, the total fraction of (100) sites increases also, although less steeply. In contrast, the fraction of (111) sites decreases slowly from 23 to 16% as the deposition varies from 0.5 to 10 C cm^{-2}. A more detailed analysis of the contribution of the various (100) sites (see Fig. 3B) indicates that the fraction of short (100) terraces increases rapidly at low deposition charge to reach a limiting value of 30% for $E_{dep} > 3$ C cm^{-2}. In contrast, the proportion of long (100) terraces increases slowly and steadily as Q_{dep} is increased from 0.5 to 10 C cm^{-2}.

To further confirm that the surface of the electrodeposited samples has a {100} preferential orientation, carbon monoxide (CO) electro-oxidation was used as a test reaction. It is well known from the literature on Pt single crystals and on oriented Pt nanoparticles that the electro-oxidation of CO is a surface structure sensitive reaction [28,38]. Indeed, on Pt surface with (100) preferential orientation, a very distinctive current peak is observed at high potential during the stripping of CO (at *ca.* 0.76 V, although the exact position of that peak varies with the sweep rate [28]). A more recent study has emphasized that issue by demonstrating that the multiplicity of the CO stripping peaks is associated to surface sites with different symmetry [39]. On well-organized Pt surfaces, the pre-peak is attributed to the presence of ordered domains with surface defects, whereas the predominant peak at 0.69 V is the sum of two anodic contributions, attributed to CO stripping from (111) sites and from low coordination sites, respectively. Finally, the peak at *ca.* 0.72 V was attributed to the oxidation of CO on (100) surface domains.

CO stripping measurements were performed at Pt thin films prepared at $E_d = -0.10$ and +0.10 V by first bubbling CO in the electrolyte while holding the electrode potential at +0.10 V. From time to time, CVs were recorded (50 mV s^{-1}) between 0.05 and 0.40 V (not shown). When stable CVs were obtained, the electrode surface was considered completely covered by CO. Following that, the excess of CO was removed by bubbling argon for 30 min, the electrode potential being kept constant at +0.10 V over that period. Then, three consecutive CVs were recorded (5 mV s^{-1}) between 0.03 and 0.80 V. In the present study, a low scan rate was used to completely remove CO molecules. During the first CV, CO stripping is performed. In all cases, the last two CVs were similar to the CVs obtained before CO adsorption, indicating that CO had been completely removed from the solution and the electrode surface. For each sample, the first CV is displayed in Fig. 4.

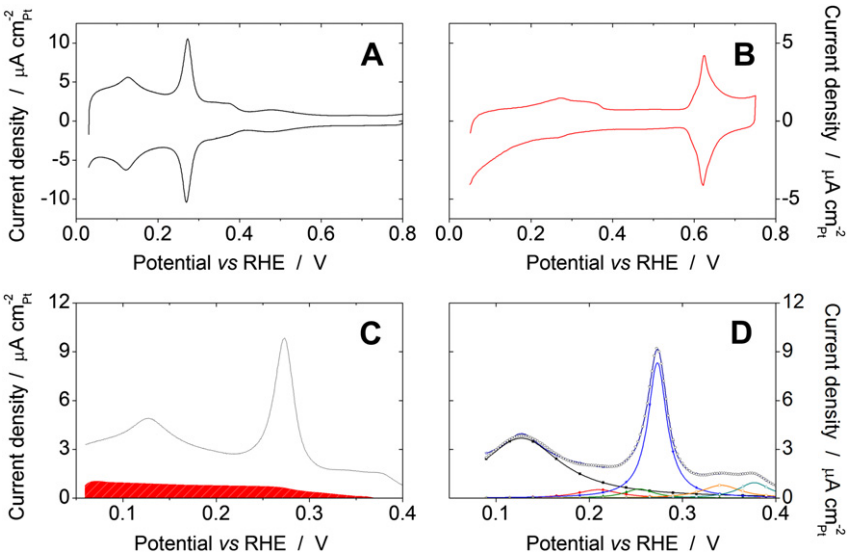

Fig. 2. Schematic representation of the deconvolution process used to assess the relative fraction of (111) and (100) surface sites on Pt electrode. In (A), blank voltammogram of the electrode in 0.5 M H_2SO_4 at 5 mV s^{-1}, (B) cyclic voltammogram in 0.5 M H_2SO_4 at 5 mV s^{-1} after Bi adsorption, (C) identification of the (111) contribution from the H-sorption region using Pt (554) as a model surface and, (D) deconvolution of the resulting profile using a series of individual contributions as described in the text.

In the case of Pt prepared at $E_d = -0.10$ V, two distinctive current peaks are observed at 0.69 and 0.72 V, with a large pre-peak that starts at potential as low as 0.35 V and that displays a plateau at *ca.* 0.50 V. The total charge under the CO stripping peak is 380 ± 10 μC cm_{Pt}^{-2}, reasonably close to the value expected for full CO coverage (460 ± 10 μC cm_{Pt}^{-2}). For Pt prepared at $E_d = +0.10$ V, a single peak is observed at 0.69 V, with a pre-peak that starts at 0.40 V. There is no distinguishable maximum to that pre-peak and it appears as a shoulder to the main oxidation peak. The CO stripping peaks appear at lower potentials than reported elsewhere due to the fact that peak potential varies with the scan rate (5 mV s^{-1} in this study) [28,33].

For Pt prepared at $E_d = -0.10$ V, the occurrence of a well-defined CO stripping pre-peak and CO stripping peak at 0.72 V clearly points to the fact that these samples contain a large fraction of ordered domains with (100) surface symmetry. The CO stripping curve of Pt thin films prepared at $E_d = +0.10$ V is clearly lacking the distinctive peak at 0.72 V, and the pre peak is poorly defined. This is coherent with the blank voltammogram in H_2SO_4 of that sample, which does not show any indication of the presence of (100) ordered domains and terraces.

Finally, the potential of zero total charge (pztc) was determined as it is known that its value varies with the surface crystallographic orientation of the electrode. To achieve this, CO adsorption was carried out by maintaining the electrode potential at +0.10 V. At this potential, the adsorption of both anions and hydrogen occurs on platinum. In brief, during the adsorption of CO, the pre-adsorbed species are displaced by CO, leading to an anodic or cathodic peak, depending if the adsorption potential is lower or higher than the pztc. So, using the total charge involved during the adsorption of CO and the blank voltammogram of the electrode, one can compute the pztc [40]. This method has been widely used for the surface characterization of platinum alloys, platinum nanoparticles and to

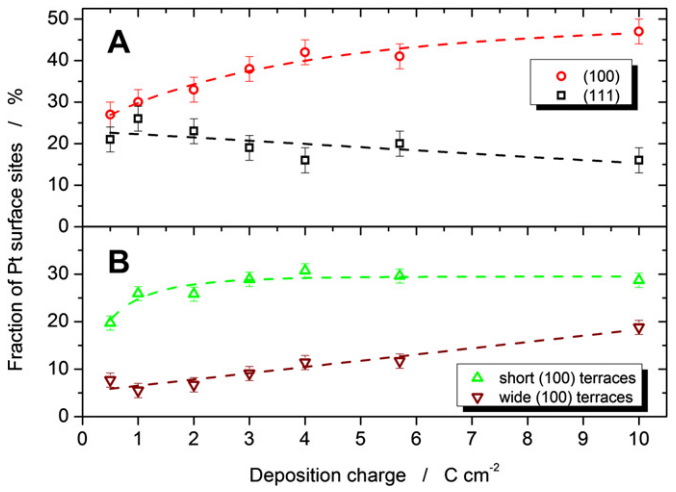

Fig. 3. In (A), variation of the total amount of (100) and (111) surface sites with the deposition charge. In (B), variation of the amount of (100) terraces and (100) step sites with the deposition charge. All Pt thin films were prepared at −0.10 V *vs* RHE.

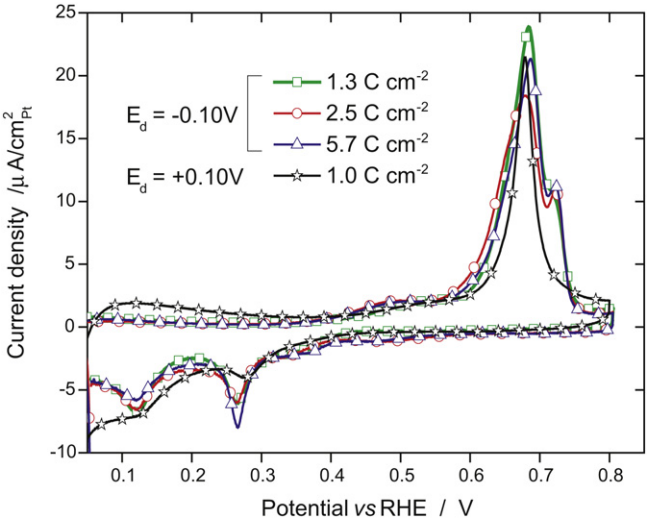

Fig. 4. CO stripping curves for Pt thin films prepared at $E_d = -0.10$ V (oriented sample) and at $E_d = 0.10$ V polycrystalline sample.

study the influence of adsorbed anions [28,40,41]. The pztc values for Pt deposited at $E_d = +0.10$ V is 255 mV, while it is 277 ± 5 mV for Pt prepared at $E_d = -0.10$ V. From the literature, the pztc value for polycrystalline Pt nanoparticles is 0.261 V, close to the value found for Pt thin films prepared at $E_d = +0.10$ V, whereas values of 0.279 V and 0.269 V were measured for Pt(100) and a (100) and (111) poly-oriented Pt electrodes, respectively [33,40]. Again, these later values are consistent with the fact that Pt electrodes prepared at $E_d = -0.10$ V have a surface showing a preferentially orientation along the {100}-axis.

Having established that Pt films prepared at $E_d = -0.10$ V contain a large fraction of (100) surface sites, it remains to explain why the percent of these (100) surface sites increases as the deposition charge is increased from 0.5 to 5.0 C cm^{-2} (see Fig. 3). The mechanism behind the growth of these preferentially oriented thin films was found to imply several factors, such as a low Pt deposition rate, low temperature and the simultaneous hydrogen evolution [31]. From the literature, it is known that adsorption of hydrogen modifies the surface free energy of the various crystallographic orientations as the enthalpy of adsorption of H_2 on the (100) surfaces is 40–60 kJ mol^{-1} higher than on (111) surfaces [42]. Therefore, while the (111) orientation of Pt is expected to be the most stable since the surface free energy varies according to $\gamma(111) < \gamma(100) < \gamma(110)$ for a face-centered-cubic metal, the surface free energy of (100) facets is the most stable in the presence of hydrogen. As discussed in detail elsewhere [31], once hydrogen is present and the thermodynamic conditions for the preferential growth of (100) facets are fulfilled, the incorporation of Pt atoms (reduction) on already present (100) facets is controlled by the kinetics of the process. In these conditions, lowering the deposition rate by decreasing the concentration of Pt cations in solution and the deposition temperature will favor the growth of (100) facets. It is not clear why the fraction of (100) surface sites increases with the deposition charge.

It is well known from the literature that the vast majority of electrocatalytic reactions is structure sensitive and the crystallographic surface orientation of the electrode profoundly affects its activity, selectivity and stability [19,43]. This is the case for ammonia and formic acid which are more easily oxidized at Pt(100) single crystals than any other surface orientation. Herein, these two surface sensitive reactions are going to be studied using Pt thin films prepared at $E_d = -0.10$ V, which were shown to exhibit a large fraction of (100) surface sites.

3.2. Performance evaluation for ammonia and formic acid electro-oxidation

Ammonia is a common waste water pollutant and a toxic gas. The oxidation of ammonia has been studied on several metal catalysts for the conception of amperometric sensor [44], to foster the development of fuel cells (ammonia can be used as a fuel in direct fuel cell applications [45] or as a high hydrogen-content fuel for in-situ hydrogen production [46]) and for environmental catalysis through the removal of ammonia from contaminated aqueous waste streams [47]. On platinum, the oxidation of ammonia has been widely studied on single crystals and nanoparticles, the results showing the extreme surface sensitivity of this reaction to the type and size of the reaction site since it takes place predominantly on (100) terraces [21,48].

Ammonia oxidation was performed in 0.2 M NaOH + 0.1 M NH_3. A high concentration of ammonia was used to reduce the influence of mass transport. Cyclic voltammograms for Pt thin films prepared at $E_d = -0.10$ V and +0.10 V and different values of Q_{dep} are shown in Fig. 5. The CVs show one main oxidation peak at *ca.* 0.67 V for the polycrystalline and at *ca.* 0.65–0.67 V for the oriented samples. At higher potentials, the current drops drastically, and no current is observed on the reverse scan. This was already attributed to either OH adsorption on the surface and/or poisoning from N_{ads} species, and will therefore not be investigated further [49].

A close inspection of the data of Fig. 5A shows the peak current value increases steadily from 136 to 212 μA cm$_{Pt}^{-2}$ as Q_d is increased from 1 to 3 C cm^{-2}. This increase in the peak current value for the electro-oxidation of NH_3 with the deposition charge can be explained from the blank voltammogram and the deconvolution performed in Figs. 1 and 3, which revealed that the fraction of (100) sites increases steadily as the deposition charge is increased from 1 to 3 C cm^{-2}. Indeed, the peak current increases linearly with the fraction of (100) surface sites for Pt thin films prepared with $1 \leq Q_d \leq 3$ C cm^{-2} (not shown). For Pt thin films prepared at $E_d = -0.10$ V and $Q_d = 5$ C cm^{-2}, the peak current decreases to 144 μA cm$_{Pt}^{-2}$ even if the fraction of (100) surface sites is higher than for films prepared with lower deposition charge (see Fig. 3). This is thought to be due to mass transfer limitation since films prepared with large Q_d are porous and are characterized by large roughness factor. Indeed, the roughness factor of Pt films ($E_d = -0.10$ V) with $Q_d = 3$ C cm^{-2} is $R_f = 38$, while that with $Q_d = 5$ C cm^{-2} is $R_f = 59$. The maximum peak current obtained for $Q_d = 3$ C cm^{-2} is up to 4.8 times higher than the one observed for polycrystalline Pt prepared at $E_d = +0.10$ V (which is 44 μA cm$_{Pt}^{-2}$), clearly highlighting the effect of the increased proportion of (100) sites on the electro-oxidation of ammonia.

To assess the long-term behavior of the various Pt thin films, chronoamperometric curves were recorded at 0.60 V. At this potential, the main product of the oxidation of NH_3 is expected to be N_2, although the formation of N_{ads}, N_2O and NO_x has been also reported at potential as low as 0.57 V [49,50]. As shown in Fig. 5B, after 1 h of operation, the current increases from 24 to 52 μA cm$_{Pt}^{-2}$ as Q_d is increased from 1 to 3 C cm^{-2} for {100}-preferentially oriented Pt sample. In comparison, the current density is only 9.5 μA cm$_{Pt}^{-2}$ for non-oriented polycrystalline Pt prepared at $E_d = +0.10$ V and $Q_d = 1$ C cm^{-2}, a factor of *ca.* 5 lower. This highlights the importance of the Pt surface orientation even on the time scale of hours. Consistently with what was observed previously, a further increase of the deposition charge ($Q_d = 5$ C cm^{-2}) decreases the current density to 39 μA cm$_{Pt}^{-2}$ due to mass transfer limitations.

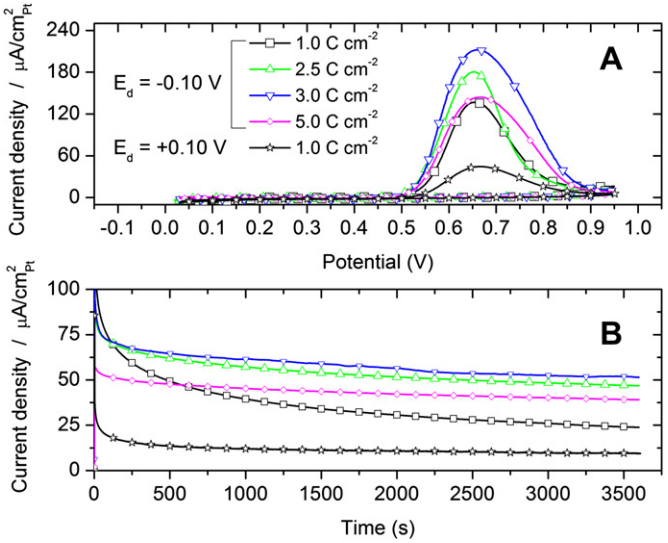

Fig. 5. In (A), cyclic voltammograms recorded at 1 mV s^{-1} in 0.1 M NH_3 + 0.2 M NaOH. In (B), chronoamperometric curves at 0.6 V in the same electrolyte.

Formic acid oxidation is of interest because it is an interesting fuel for polymer electrolyte fuel cells [51,52]. The voltammetric responses for HCOOH oxidation are shown in Fig. 6A. For polycrystalline Pt, negligible current is observed on the forward scan until the electrode potential reaches *ca.* 0.75 V, which is due to the fact that oxidation of HCOOH leads to the adsorption of CO that rapidly poisons the surface. At higher potentials, CO is oxidized and formic acid oxidation occurs to a significant extent, giving rise to a current increase. On the reverse scan, a stable current of *ca.* 0.5 mA cm_{Pt}^{-2} is observed until the electrode potential reaches 0.55 V. At lower potentials, the current slowly decreases due to CO poisoning of the electrode surface until a negligible value is reached below 0.3 V.

The CV of the preferentially oriented {100} Pt samples does not differ much from that of polycrystalline Pt except for the intensity of the current observed in the different potential regions. Indeed, a limited current is observed on the forward scan until the electrode potential reaches *ca.* 0.75 V, where the current increases sharply. However, on the reverse scan, a much higher current is observed, which reaches 1.30 and 0.97 mA cm_{Pt}^{-2} for Q_d = 2 and 5 C cm^{-2}, respectively. Again, the lower activity for the Q_d = 5 C cm^{-2} sample might be due to mass transfer limitations as it was observed previously for ammonia oxidation. In comparison, for the Pt polycrystalline sample prepared at $E_d = +0.10$ V, the maximum current is 0.50 mA cm^{-2}, which is a factor of 2.6 lower than the maximum current observed for the preferentially oriented {100} Pt sample. This is consistent with the fact that Pt (100) single crystals have the highest intrinsic activity for formic acid oxidation [4].

To assess the long-term behavior of the various Pt thin films, chronoamperometric curves were recorded at 0.4 V (Fig. 6B). For short time electrolysis (less than *ca.* 300 s), the activity trend is maintained, and the current density of the preferentially oriented {100} Pt samples with Q_d = 2 and 5 C cm^{-2} is 86 and 57 μA cm^{-2}, respectively, compared to 21 μA cm^{-2} for polycrystalline Pt. However, for longer period of electrolysis (*ca.* 1800 s), the currents of all samples are the same (7.3 μA cm_{Pt}^{-2}), independent of the deposition potential and deposition charge used during the preparation of the films. Again, this is consistent with the fact that, although Pt(100) is the most active crystallographic orientation for formic acid oxidation, it is also the most easily poisoned by CO, therefore explaining why all Pt thin films tend toward the same current value if the electrolysis of formic acid is prolonged over a long period of time. In order to exploit the full benefit of porous and preferentially oriented {100} Pt electrodes, it will be necessary to improve the tolerance to poisoning via the use of adatoms and/or formation of alloy.

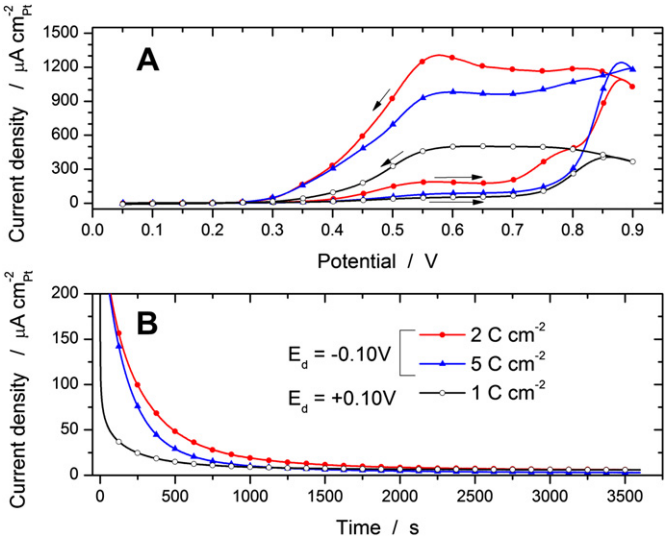

Fig. 6. In (A), cyclic voltammograms recorded at 5 mV s^{-1} in 0.5 M HCOOH + 0.5 M H_2SO_4. In (B), chronoamperometric curves at 0.4 V in the same electrolyte.

4. Conclusion

Highly {100}-oriented Pt thin films were prepared by electrodeposition through a potentiostatic method without the use of any surfactants. Bismuth oxidation and deconvolution of the hydrogen desorption peaks allowed us to proceed to a precise determination of the amount of (111) and (100) surface sites. Pt thin films prepared at $E_d = -0.10$ V with a low deposition charge (Q_{dep} = 1 C cm^{-2}) exhibits a low roughness factor (R_f = 7) and 26% of their surface sites have an (100) orientation, while films prepared at the same potential but with a large deposition charge (Q_{dep} = 5 C cm^{-2}) have a high roughness factor (R_f = 46) and a much higher (47%) fraction of (100) surface sites. Also, it was shown that the balance between (100) terraces and (100) step sites varies with the deposition charge, with the (100) terraces being favored as the deposition charge is increased. The occurrence of a preferential orientation on Pt thin films prepared at $E_d = -0.10$ V is confirmed by CO stripping curves, that exhibit a very distinctive pre-peak at *ca.* 0.50 V and sharp peak at 0.72 V, and by a potential of zero total charge of 277 mV *vs* RHE, close to the value of 279 mV reported for Pt (100) single crystal.

To demonstrate the interest of these preferentially oriented {100} Pt electrodes, their activities for the electro-oxidation of ammonia and formic acid was assessed by cyclic voltammetry and chronoamperometric measurements. It was shown that the occurrence of Pt (100) surface sites leads to a factor of 4.8 and 2.6 increase of the current (expressed as μA cm_{Pt}^{-2}) for the oxidation of ammonia and formic acid, respectively.

Acknowledgment

This work was supported by the Natural Sciences and Engineering Research Council of Canada (NSERC) and the Canada Research Chair program. Also, one of us (EB) would like to acknowledge the financial support of NSERC through an Alexander Graham Bell Canada Graduate Scholarship (CGS) (Master degree) and the Michael Smith Foreign Study Supplements program, as well as the Fond Québécois de la Recherche sur la Nature et les Technologies (FQRNT) through the master research scholarships (B1) program.

References

[1] V. Rosca, M.T.M. Koper, Electrochim. Acta 53 (2008) 5199–5205.
[2] V. Rosca, M.T.M. Koper, Phys. Chem. Chem. Phys. 8 (2006) 2513–2524.
[3] V. Grozovski, J. Solla-Gullón, V. Climent, E. Herrero, J.M. Feliu, J. Phys. Chem. C 114 (2010) 13802–13812.
[4] J. Solla-Gullón, F.J. Vidal-Iglesias, A. López-Cudero, E. Garnier, J.M. Feliu, A. Aldaz, Phys. Chem. Chem. Phys. 10 (2008) 3689–3698.
[5] E. Antolini, J.R.C. Salgado, E.R. Gonzalez, Appl. Catal. B Environ. 63 (2006) 137–149.
[6] E. Antolini, Mater. Chem. Phys. 78 (2003) 563–573.
[7] A. Chen, P. Holt-Hindle, Chem. Rev. 110 (2010) 3767–3804.
[8] A. Ponrouch, S. Garbarino, D. Guay, Electrochem. Commun. 11 (2009) 834–837.
[9] L. Liu, E. Pippel, R. Scholz, U. Gosele, Nano Lett. 9 (2009) 4352–4358.
[10] J. Zhang, F.H.B. Lima, M.H. Shao, K. Sasaki, J.X. Wang, J. Hanson, R.R. Adzic, J. Phys. Chem. B 109 (2005) 22701–22704.
[11] X. Zhao, M. Yin, L. Ma, L. Liang, C. Liu, J. Liao, T. Lu, W. Xing, Energy Environ. Sci. 4 (2011) 2736–2753.
[12] S. Guo, E. Wang, Nano Today 6 (2011) 240–264.
[13] Y. Bing, H. Liu, L. Zhang, D. Ghosh, J. Zhang, Chem. Soc. Rev. 39 (2010) 2184–2202.
[14] C. Hamel, S. Garbarino, E. Irissou, M.-P. Bichat, D. Guay, J. Phys. Chem. C 114 (2010) 18931–18939.
[15] S. Koh, J. Leisch, M.F. Toney, P. Strasser, J. Phys. Chem. C 111 (2007) 3744–3752.
[16] S. Garbarino, A. Ponrouch, S. Pronovost, D. Guay, Electrochem. Commun. 11 (2009) 1449–1452.

[17] E. Bertin, S. Garbarino, A. Ponrouch, D. Guay, J. Power Sourc. 206 (2012) 20–28.
[18] P. Bommersbach, M. Chaker, M. Mohamedi, D. Guay, J. Phys. Chem. C 112 (2008) 14672–14681.
[19] J. Solla-Gullón, F.J. Vidal-Iglesias, J.M. Feliu, Annu. Rep. Prog. Chem., Sect. C Phys. Chem. 107 (2011) 263–297.
[20] F.J. Vidal-Iglesias, N. Garcia-Araez, V. Montiel, J.M. Feliu, A. Aldaz, Electrochem. Commun. 5 (2003) 22–26.
[21] F.J. Vidal-Iglesias, J. Solla-Gullón, V. Montiel, J.M. Feliu, A. Aldaz, J. Phys. Chem. B 109 (2005) 12914–12919.
[22] R.M. Cervino, W.E. Triaca, A.J. Arvia, J. Electroanal. Chem. 182 (1985) 51–60.
[23] J. Gomez, L. Vazquez, A.M. Baro, N. Garcia, C.L. Perdriel, W.E. Triaca, A.J. Arvia, Nature 323 (1986) 612–614.
[24] W.E. Triaca, A.J. Arvia, J. Appl. Electrochem. 20 (1990) 347–356.
[25] T.S. Ahmadi, Z.L. Wang, T.C. Green, A. Henglein, M.A. El-Sayed, Science 272 (1996) 1924–1925.
[26] T.S. Ahmadi, Z.L. Wang, A. Henglein, M.A. El-Sayed, Chem. Mater. 8 (1996) 1161–1163.
[27] J. Solla-Gullón, P. Rodríguez, E. Herrero, A. Aldaz, J.M. Feliu, Phys. Chem. Chem. Phys. 10 (2008) 1359–1373.
[28] J. Solla-Gullón, F.J. Vidal-Iglesias, E. Herrero, J.M. Feliu, A. Aldaz, Electrochem. Commun. 8 (2006) 189–194.
[29] S. Brimaud, S. Pronier, C. Coutanceau, J.M. Léger, Electrochem. Commun. 10 (2008) 1703–1707.
[30] I. Bakos, G. Horanyi, J. Electroanal. Chem. 397 (1995) 105–110.
[31] A. Ponrouch, S. Garbarino, E. Bertin, C. Maunders, G.A. Botton, D. Guay, Adv. Funct. Mater. 22 (2012) 4172–4181.
[32] P. Perret, T. Brousse, D. Belanger, D. Guay, J. Electrochem. Soc. 156 (2009) A645–A651.
[33] Q.-S. Chen, J. Solla-Gullón, S.-G. Sun, J.M. Feliu, Electrochim. Acta 55 (2010) 7982–7994.
[34] S. Garbarino, A. Ponrouch, S. Pronovost, J. Gaudet, D. Guay, Electrochem. Commun. 11 (2009) 1924–1927.
[35] E. Bertin, C. Roy, S. Garbarino, D. Guay, J. Solla-Gullón, F.J. Vidal-Iglesias, J.M. Feliu, Electrochem. Commun. 22 (2012) 197–199.
[36] S. Garbarino, A. Ponrouch, E. Bertin, D. Guay, MRS Online Proc. Lib. 1311 (2011) GG06–GG17.
[37] P. Rodríguez, J. Solla-Gullón, F.J. Vidal-Iglesias, E. Herrero, A. Aldaz, J.M. Feliu, Anal. Chem. 77 (2005) 5317–5323.
[38] A. Cuesta, A. Couto, A. Rincón, M.C. Pérez, A. López-Cudero, C. Gutiérrez, J. Electroanal. Chem. 586 (2006) 184–195.
[39] P. Urchaga, S. Baranton, C. Coutanceau, G. Jerkiewicz, Langmuir 28 (2012) 3658–3663.
[40] T.-Y. Jeon, S.J. Yoo, Y.-H. Cho, K.-S. Lee, S.H. Kang, Y.-E. Sung, J. Phys. Chem. C 113 (2009) 19732–19739.
[41] A. López-Cudero, A. Cuesta, C. Gutiérrez, J. Electroanal. Chem. 548 (2003) 109–119.
[42] N.M. Marković, P.N. Ross Jr., Surf. Sci. Rep. 45 (2002) 117–229.
[43] V. Rosca, M. Duca, M.T. DeGroot, M.T.M. Koper, Chem. Rev. 109 (2009) 2209–2244.
[44] B.A. Lopez De Mishima, D. Lescano, T. Molina Holgado, H.T. Mishima, Electrochim. Acta 43 (1998) 395–404.
[45] S. Suzuki, H. Muroyama, T. Matsui, K. Eguchi, J. Power Sourc. 208 (2012) 257–262.
[46] F. Vitse, M. Cooper, G.G. Botte, J. Power Sourc. 142 (2005) 18–26.
[47] G. Perez, J. Saiz, R. Ibanez, A.M. Urtiaga, I. Ortiz, Water Res. 46 (2012) 2579–2590.
[48] F.J. Vidal-Iglesias, J. Solla-Gullón, P. Rodríguez, E. Herrero, V. Montiel, J.M. Feliu, A. Aldaz, Electrochem. Commun. 6 (2004) 1080–1084.
[49] F.J. Vidal-Iglesias, J. Solla-Gullón, J.M. Feliu, H. Baltruschat, A. Aldaz, J. Electroanal. Chem. 588 (2006) 331–338.
[50] A.C.A. de Vooys, M.T.M. Koper, R.A. van Santen, J.A.R. van Veen, J. Electroanal. Chem. 506 (2001) 127–137.
[51] V. Grozovski, V. Climent, E. Herrero, J.M. Feliu, Chem. Phys. Chem. 10 (2009) 1922–1926.
[52] X. Yu, P.G. Pickup, J. Power Sourc. 182 (2008) 124–132.